Measurement 175 (2021) 109136

Contents lists available at ScienceDirect

Measurement

journal homepage: www.elsevier.com/locate/measurement

Nonlinear vibration analysis of nanowire resonators for ultra-high resolution mass sensing

Rosa Fallahpour [a,*], Roderick Melnik [a,b]

[a] The MS2Discovery Interdisciplinary Research Institute, M²NeT Laboratory, Wilfrid Laurier University, Waterloo, ON, N2L 3C5, Canada
[b] BCAM-Basque Center for Applied Mathematics, Alda. Mazarredo, E-48009, Bilbao, Spain

ARTICLE INFO

Keywords:
Nonlinear vibrations
Nanowire
Ultra-high resolution
Mass sensor
Thermal effects

ABSTRACT

Nanoscale systems fabricated with low-dimensional nanostructures such as carbon nanotubes, nanowires, quantum dots, and more recently graphene sheets, have fascinated researchers from different fields due to their extraordinary and unique physical properties. For example, the remarkable mechanical properties of nanowires empower them to have a very high resonant frequency up to the order of giga to terahertz. In this paper, we originally propose a nonlinear model for the vibrations of piezoelectric nanowire resonators with added mass considering thermal variation, electromagnetic field, surface effects, external excitation, and nonlinear foundation. The mathematical model for such nanowires is formulated by applying the Euler–Bernoulli beam theory in conjunction with the nonlocal differential constitutive relations of Eringen type. In order to analyze the obtained nonlinear partial differential equation (PDE), we first use the Galerkin method in combination with a perturbation technique to obtain the primary and super-harmonic resonances. After finding the resonance cases, a parametric sensitivity analysis is carried out to investigate the effects of key parameters on the sensitivity of the nanowire resonators in mass sensing. Our main hypothesis is that tiny particles attached to the surface of the nanowire resonator would result in a detectable shift in the value of the jump frequency. The sensitivity analysis shows that the nanowire resonator is capable of detecting added mass in the order of zeptogram. In addition, we have developed a system identification technique based on the proposed mathematical model for the detection of tiny mass rested on the nanowire resonator that we have analyzed. Furthermore, a molecular dynamic simulation study has been presented to qualitatively verify the hypothesis of frequency shift due to the added mass. The results demonstrate a high potential of nanowire resonators in detecting tiny bio-particles such as DNA, RNA, proteins, viruses, and bacteria.

1. Introduction

Detection of tiny objects such as DNA, RNA, proteins, viruses, and bacteria is very important for preventing, accurate diagnosing and effective curing different types of diseases. Accordingly, it is crucial to develop novel, practical, and effective techniques to detect tiny bio-objects. This important and interdisciplinary subject has prompted scientists, engineers, and applied mathematicians to propose and investigate innovative approaches for the detection of bio-objects. Recent years have witnessed rapid advances in the development of nanodevices for different applications such as self-powered sensing, energy harvesting and mass sensing with potential of bio-object detection. Several nanoresonators have been designed, modeled, optimized and fabricated for tiny mass sensing. These nanoresonators are made of carbon nanotubes, graphene sheets, and nanowires (NWs) [1–3]. Due to their ultra-high modulus of elasticity and resonant frequency, they received substantial attention of the researchers as they can be used as sensors for label-free detection of specific biological objects. Although a number of important studies have been undertaken in this field so far, in particular those aiming to implement nanoresonators for bio-object detection [4–6], there is still lack of robust and systematic modeling techniques for the nanoresonators. Specifically, it concerns the application of nanowires in biological detection, taking into account some of the most important parameters. These include parameters connected with electromagnetic fields, thermal variations, external excitations, axial loads, nonlocal and surface effects, large oscillations, and nonlinear viscoelastic foundations. Having in mind applications in mass detection, it is highly important to develop a mathematical model, which can be used to investigate the effect of these parameters on the frequency behavior of nanowires. In fact, the outstanding capability

* Corresponding author.
E-mail addresses: rosa.fp68@gmail.com (R. Fallahpour), rmelnik@wlu.ca (R. Melnik).

https://doi.org/10.1016/j.measurement.2021.109136
Received 11 September 2020; Received in revised form 5 January 2021; Accepted 1 February 2021
Available online 10 February 2021
0263-2241/© 2021 Elsevier Ltd. All rights reserved.

of nanomechanical resonators, specially nanowires for ultra-high resolution mass sensing applications, is largely related to their dynamic characteristics [7].

The utilization of continuum theories for the modeling of vibrations of nanoresonators has been popular among the researchers in this field [8,9]. Modeling of nanoresonators are categorized in two different themes. In the first theme, the focus of researchers is on the use of different continuum theories such as Timoshenko, Euler–Bernoulli and Rayleigh to model vibrations of nanostructures such as nanowires [10,11]. Based on their investigations regarding the continuum theories, researchers have considered different effects such as thermal variations and piezoelectric potential to model vibrations of nanowires. In addition, a few researchers have combined classical and nonlocal beam theories to characterize the dynamics of nanowires. Using these combined models, they investigated the effect of different parameters such as size, surface and nonlocal parameters on the vibrations of nanowires [12,13]. The second theme is based on the models with focus on the applications of nanoresonators in mass sensing, biological detection and drug delivery [14,15]. Similar to the first category of research in this area, researchers have used classical and non-classical theories to study the applications and potency of the nanowire resonators for the detection of tiny bio-objects and chemical atoms [16,17].

The use of continuum models for the vibrations analysis of nanowires started from the early 2000s (e.g. [18] and references therein). The main aim of most of the published works on the vibrations of nanowires at that time was finding a closed-form representation for the natural frequency of the nanowires, and also providing a mathematical framework to predict the behavior of nanowires under different cases of oscillations. The focus of earlier research on this topic was on the development of one-dimensional vibration models to obtain the natural frequencies of nanowires considering the electrostatic effect, while using classical beam theories. One of the earliest efforts on modeling vibrations of nanowires was presented by Ustunel et al. [19] in which the authors proposed a one-dimensional model for NWs. In another pioneering work, Vincent et al. [20] studied self-sustained vibrations of nanowires under a constant electron beam . In an interesting work by Zhou et al. vibrations of zinc oxide nanowires were studied considering the electric field effects. Their developed partial differential equation was converted to a nonlinear ordinary differential equation with both quadratic and cubic nonlinearities [10].

Another path of research in this field has been the consideration of nonlocal and surface effects in the vibrations of nanowires. One of the earliest attempts in which a continuum model was proposed for the vibration analysis of nanowires was a paper by He and Liley where they developed a model for the vibrations of NWs considering surface effects and different boundary conditions [13]. Effects of surface stress on both buckling and vibrations of piezoelectric nanowires were studied by Wang and Feng in 2010 [12]. They showed that the resonant frequency of piezoelectric nanowires can be adjusted using the applied electric potential. They also demonstrated that piezoelectricity and the surface stress have quite similar effects on the frequency response of the nanowire [12]. Kiani in one of his early research papers in this area [21], developed a nonlocal continuum model to study free longitudinal vibrations of tapered nanowires employing the perturbation techniques. In this study, he considered two different types of boundary conditions including fixed–fixed and fixed–free constraints. One of the main results of the research was related to the rate of change in NW radii. For higher values of the small scale effect parameter, the rate of change in radii is more pronounced on the variation of the natural frequencies and phase velocities [21]. Hasheminejad and Gheshlaghi [22] developed a dissipative surface stress model to investigate the influence of size-dependent surface dissipation on fundamental frequencies of nanowires. Euler–Bernoulli beam theory in conjunction with the classic Zener model was used to develop the fifth order differential equation, which describes the flexural vibrations of NWs. Fu et al. [23] studied nonlinear free vibrations of NWs using nonlocal Timoshenko beam theory considering the surface effects. Askari and Esmailzadeh used nonlocal Timoshenko beam theory to study vibrations of nanowires considering geometrical nonlinearity and different surface areas using the variational iteration method [24]. He and Lilley investigated the vibrations of nanowires considering the surface effects and using the Timoshenko beam theory. They obtained the quality factor of nanowire's vibrations, and showed that considering the surface stress decreases the stiffness of cantilever nanowire, and increases the stiffness of nanowires with simply supported boundary conditions [25]. Samaei et al. [26] studied vibrations of piezoelectric nanowires considering surface effects. They developed a continuum model for the vibrations of nanowires, which takes into account the effects of surface elasticity, residual surface tension, and transverse shear deformation. The main conclusions of their work is that the surface effects increase the natural frequency for the lower modes.

A few researchers have developed models for the vibrations of nanowires considering external excitations, elastic foundations and nonlinearity. For example, both free and forced vibrations of nanowire rested on an elastic substrate were studied by Su et al. They assumed Winkler–Pasternak foundations and generalized substrate models as the foundation model for the nanowire [11]. In their work, they obtained the characteristic equations, mode shapes and effective Young's moduli of the nanowires considering different forms of boundary conditions [11]. In another research [27], free and forced transverse vibrations of nanowires were studied taking into account the surface effects based on the Timoshenko beam theory. A comparison study was also performed by the authors to verify the obtained theoretical results for the fundamental frequencies with the FEM simulation [27]. Zhang et al. in [28] analyzed transverse vibrations of embedded nanowires under axial compression taking into account the higher order surface effects. Jin and Li studied nonlinear dynamics of silicon nanowire (SiNW) considering nonlocal effects. They performed a bifurcation analysis, which shows that the nonlocal effect causes the most significant impact when the excitation frequency equals to the natural frequency of the structure [29]. Sedighi and Bozorgmehri probed nonlinear vibrations along with adhesion instability of nonlocal nanowires with consideration of surface energy. They revealed that the critical Casimir value decreases by increasing the nonlocal parameter [30].

In recent studies, researchers have also focused on irregular geometries of nanowire resonators. For example, Khosravi et al. [31] developed a vibration model for the torsional vibration of a triangular nanowire resonator. They showed that the triangular edge as well as the nonlocal parameter have an inverse impact on the natural frequency. In another research, Yuan et al. [32] studied torsional vibration of non-prismatically non-homogeneous nanowires with multiple defects. They showed that the nonlocality effect lessens by growing the nanowire's length.

In the present paper, we originally study the effect of temperature variations and electromagnetic fields effect on the sensitivity of piezoelectric nanowire-based resonators with application to ultra-high resolution mass sensing. Using the nonlocal Euler–Bernoulli beam theory and considering the surface effect, a mathematical model is developed for the nanowire resonators. A nonlinear Winkler foundation along with Pasternak coefficient are assumed for the oscillating nanowire resonator. Furthermore, a large oscillation term, which results in nonlinearity, is considered for the vibrations of the considered system. It is supposed that the nanoresonator is triggered with a periodic force. In addition, the proposed mathematical model for the vibrations of nanoresonators includes a term relevant to the added mass, which can be considered as a tiny bio-object such as virus. In order to investigate the nanoresonators principal mode of vibrations, the Galerkin method is implemented, and accordingly, a corresponding nonlinear ordinary differential equation is obtained. The Method of Multiple Scales (MMS) is used to find the primary resonance of the nanoresonator, then its sensitivity is investigated to the tiny added mass based on the analysis

of the jump phenomenon in the scale of zeptogram. It should be noted that there are several semi-analytical and numerical approaches for analyzing nonlinear oscillatory systems. Among these techniques, MMS has shown an excellent capability in the analysis of nonlinear characteristics such as jump phenomenon. Another interesting point about the MMS is its sufficient accuracy for qualitative analysis based on its first approximation. This method tackles the shortcomings of other classical techniques such as the Poincare–Lindstedt method and the straightforward expansion with two important advantages. First, introducing scaled space and time coordinate in MMS technique helps in capturing the slow pattern modulation. Secondly, we can obtain the solvability condition based on secular terms. A molecular dynamic simulation is also presented in this paper to verify the hypothesis of frequency shift of nanowire resonators based on added mass.

The main contributions of the present research are the development of a novel mathematical model for the vibrations of nanowire resonators, and a comprehensive analysis of frequency shifts owing to added mass to nanowire resonators using primary, sub-harmonic, and super-harmonic resonances. In addition, a new efficient online parameter identification technique based on the developed model for the tiny mass detection has also been proposed.

2. Mathematical modeling

In this section, we aim to model the vibrations of piezoelectric nanowires, taking into account electromagnetic, thermal, nonlocal and surface effects with an external load rested on a Winkler foundation [33]. Fig. 1(a) shows the geometry of the considered nanowire resonator in this paper. The trajectories with violet and blue colors represent the magnetic fields in Fig. 1(a) and Fig. 1(c), respectively. There exist different types of nanowire resonators with distinct forms of cross sections such as circular and rectangular. In our model, it is supposed that the nanowire has a rectangular cross section as it can provide a flat surface on its top for locating the added mass, comparing to the circular cross section. The nanowire resonator has the length of L, height of $2h$, and width of b, as indicated in Fig. 1(b). Fig. 1(c) represents a 3D view of the nanowire resonator. In the first approximation, we will represent our nanowire as a beam.

Based on the Euler–Bernoulli beam theory (EBT), the displacement field of a nanowire can be found by the following equations:

$$u_a = u(x,t) - z\frac{\partial w(x,t)}{\partial x}, \qquad u_b = 0, \qquad u_c = w(x,t), \tag{1}$$

in which u and w represent the axial and transverse deflection, respectively. According to the nonlinear von Karman theory [34], the only nonzero strain of the Euler–Bernoulli beam theory is as following:

$$\epsilon_{xx} = \frac{\partial u(x,t)}{\partial x} + \frac{1}{2}\left(\frac{\partial w(x,t)}{\partial x}\right)^2 - z\frac{\partial^2 w(x,t)}{\partial x^2}, \tag{2}$$

where ϵ_{xx} is the strain in x direction.

In accordance with the EBT, we have the following relations between transverse shear forces V, bending moment M and the axial forces N:

$$\frac{\partial V(x,t)}{\partial x} = \frac{\partial^2 M(x,t)}{\partial x^2} + N(x,t)\frac{\partial^2 w(x,t)}{\partial x^2}, \tag{3}$$

and

$$\frac{\partial N(x,t)}{\partial x} + f_u = 0, \tag{4}$$

where f_u is the distributed axial load (measured per unit undeformed length) [35–37]. Based on the nonlocal theory, we can write:

$$\Xi(\sigma_{xx}) = E\epsilon_{xx}, \qquad \Xi(\sigma_{xz}) = 2G\epsilon_{xz}, \qquad \Xi = 1 - \Gamma\frac{\partial^2}{\partial x^2}, \tag{5}$$

in which E is the Young modulus and G represents shear modulus. Γ implies the nonlocal parameter, which is equal to zero in the local theory.

Following [36,38], we have the axial force–strain relation, which is identical in all beam theories:

$$\Xi(N) = N - \Gamma\frac{\partial^2 N}{\partial x^2} = EA\left[\frac{\partial u}{\partial x} + \frac{1}{2}\left(\frac{\partial w}{\partial x}\right)^2\right], \tag{6}$$

and

$$A = \int_A dA, \qquad \int_A z dA = 0,$$

where the x axis passes through the geometric centroid of the beam.

Accordingly, the constitutive relationship between bending moment and strain is constructed as below [38]:

$$M - \Gamma\frac{\partial^2 M}{\partial x^2} = -EI\frac{\partial^2 w}{\partial x^2}. \tag{7}$$

Extending the nonlocal theory to piezoelectric material, one could have:

$$\sigma_n = \int_V K(|x'-x|,\tau_m)[C\epsilon_t(x') - eE_e(x')]dx, \tag{8}$$

$$D = \int_V K(|x'-x|,\tau_m)[e\epsilon_t(x') - \in E_e(x')]dx. \tag{9}$$

The differential constitutive equations corresponding to the integral form of Eqs. (8) and (9), can be reconstructed as below:

$$\sigma_n - \Gamma\ \nabla^2\sigma_n = C\epsilon_t - eE_e, \tag{10}$$

$$D - \Gamma\ \nabla^2 D = e\epsilon_t + \lambda E_e, \tag{11}$$

in which D, E_e, C, e and λ are electric displacement, electric field, fourth-order elasticity tensor, piezoelectric constants and dielectric constants, respectively.

In order to develop the mathematical model of the considered nanoresonator, we need to find the corresponding axial load N, shear force V, and bending moment M. This will lead us to having all required mechanical terms in Eq. (3) based on the Euler–Bernoulli beam theory. In addition, as we are using nonlocal theory, it is required to use all equations described in Eq. (5) to Eq. (11).

We first start with modeling the surface effects in our nanowire resonator. As we deal with a nanoresonator, due to the small ratio of the volume to area, it is important to account for the surface effects in the modeling in order to be able to carry out a more practical and accurate analysis of the mass sensitivity of the nanowire resonator. The surface stresses of the nanowire can be described by the following equation:

$$\sigma_{xz} = \tau_0\frac{\partial w}{\partial x}. \tag{12}$$

As it is required to fully satisfy the equilibrium conditions between nanowire's main core and corresponding surface layers, the following equations for both the upper and lower surfaces must be satisfied [39]:

$$\sigma^{up}_{mj,m} - \sigma^{up}_{jz} = \rho_0\frac{\partial^2 u^{up}_j}{\partial t^2}, \qquad \sigma^{l}_{mj,m} + \sigma^{l}_{jz} = \rho_0\frac{\partial^2 u^{l}_j}{\partial t^2}, \tag{13}$$

where the up and l signs represent the upper and lower surfaces, respectively, ρ_0 is the surface density of surface layers. We have $m = x, y$ and $j = x, y, z$. Considering Eqs. (1) and (12), Eq. (13) can be reconstructed for the transverse vibrations of the nanowire as follows [39]:

$$\sigma^{up}_{zz} = \tau_0\frac{\partial^2 w}{\partial x^2} - \rho_0\frac{\partial^2 w}{\partial t^2}, \qquad \sigma^{l}_{zz} = -\tau_0\frac{\partial^2 w}{\partial x^2} + \rho_0\frac{\partial^2 w}{\partial t^2}. \tag{14}$$

The following equation displays the linear variation of σ_{zz} through the nanowire thickness:

$$\sigma_{zz} = \frac{1}{2}(\sigma^{up}_{zz} + \sigma^{l}_{zz}) + \frac{z}{2h}(\sigma^{up}_{zz} - \sigma^{l}_{zz}). \tag{15}$$

Substituting Eq. (14) into Eq. (15), results in the following equation for σ_{zz} :

$$\sigma_{zz} = \frac{z}{h}\left(\tau_0\frac{\partial^2 w}{\partial x^2} - \rho_0\frac{\partial^2 w}{\partial t^2}\right). \tag{16}$$

Based on the Laplace–Young equation, we assume two distributed loads are exerted along the x coordinate due to the effect of residual

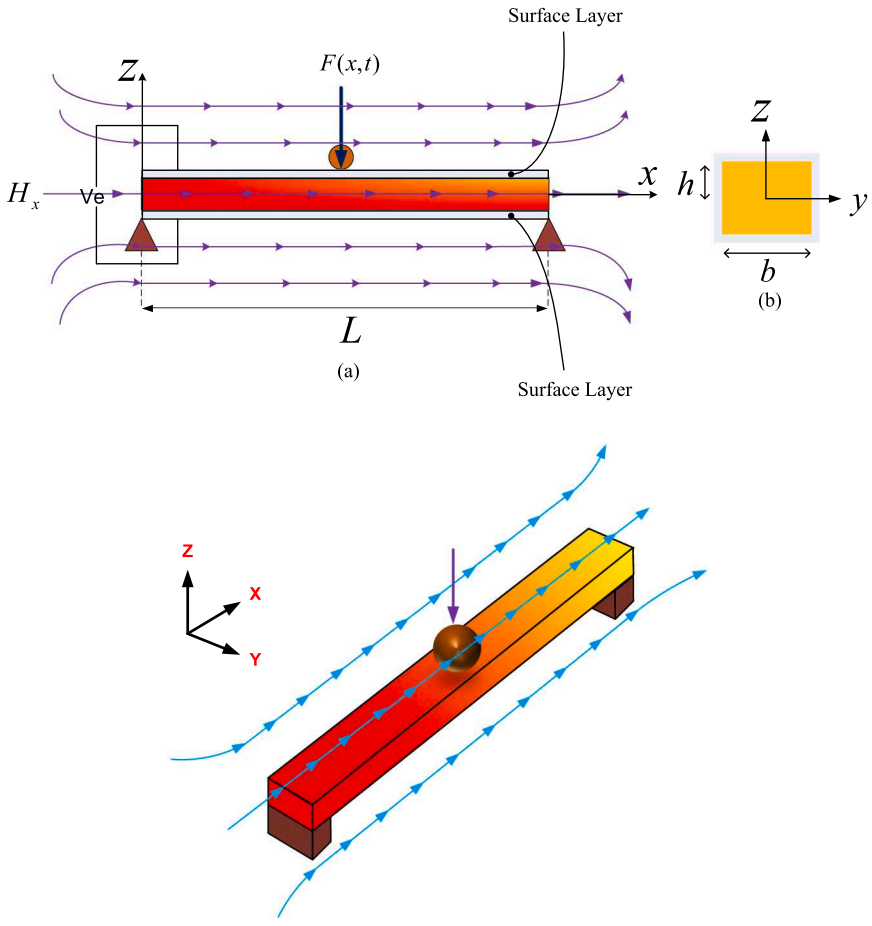

Fig. 1. Schematic of the nanoresonator, (a) a piezoelectric nanowire under harmonic load, thermal and electromagnetic fields effects, (b) cross section of the nanowire, (c) 3D view of the nanowire resonator.

surface stress. Accordingly, the following forms are considered for the distributed loads pertinent to the surface stress effects:

$$g_1(x) = b\tau_0^{up}\frac{\partial^2 w}{\partial x^2}, \qquad g_2(x) = b\tau_0^{l}\frac{\partial^2 w}{\partial x^2}. \tag{17}$$

It is supposed that, both upper and lower surfaces have analogous properties, therefore, the resultants of the above-mentioned distributed loads are presented as below [39]:

$$G_s(x) = g_1(x) + g_2(x) = 2b\tau_0\frac{\partial^2 w}{\partial x^2}. \tag{18}$$

Temperature variations can change the sensitivity of the nanowire resonator for mass sensing. For understanding the effect of thermal variations on the response of the nanowire resonator, we should consider the exerted stress due to the thermal load in our modeling. In order to account for the thermal effect in our model, we need to add the thermal stress–strain term to Eq. (2). The thermal stress term can be written as follows:

$$\sigma_\theta = -\frac{E}{1-2\upsilon}\alpha_x\theta_t, \tag{19}$$

where σ_θ, ν, α_x, and θ_t represent the axial thermal stress, Poisson ratio, the coefficient of thermal expansion in the direction of x axis, and temperature, respectively. Accounting for large amplitudes of oscillations of the nanowire and the axial load due to the thermal stress, we have the following relation for the longitudinal displacement u as a function of transverse deformation w [40]:

$$u = -\frac{1}{2}\int_0^L\left(\frac{\partial w}{\partial x}\right)^2 dx + \frac{x}{2L}\int_0^L\left(\frac{\partial w}{\partial x}\right)^2 dx - \frac{1}{2}\int_0^L\left(\frac{1}{1-2\upsilon}\right)\alpha_x\theta_t dx. \tag{20}$$

Substituting Eqs. (2) and (20) into Eq. (4) results in:

$$T = \frac{EA}{2L}\left(\int_0^L\left(\frac{\partial w}{\partial x}\right)^2 dx - \frac{1}{1-2\upsilon}\alpha_x\theta_t\right), \tag{21}$$

where T represents two terms of the axial load owing to thermal stress and the large oscillations of the nanowire.

Another important term that should be taken into account is the electromagnetic field effect. Several researchers have shown that the magnetic field is affecting the vibrations of nanowire [41]. In accordance with this observation, it is critical to take into account the effect of electromagnetic field in our modeling of nanowire resonators with application in mass sensing. As we only investigate the transverse vibrations of the nanowire, the Lorentz force in z-direction is implemented as:

$$f_{em} = f_z = \zeta_m H_x^2\frac{\partial^2 w}{\partial x^2}. \tag{22}$$

The above equation is used in our governing equation of the transverse vibration, Eq. (34), as the term for electromagnetic force. The mathematical procedure for finding this equation can be found in Appendix A.

For the piezoelectric effect, we should find its corresponding axial load. Accordingly, the electric displacement can be given by the following equations [42,43]:

$$E_x = -\frac{\partial\psi}{\partial x}, \qquad E_z = -\frac{\partial\psi}{\partial z}, \tag{23}$$

and we have:

$$D_x = \lambda_{11} E_x, \qquad D_z = e_{31}\epsilon_{xx} + \lambda_{33} E_z, \tag{24}$$

$$\frac{\partial D_x}{\partial x} + \frac{\partial D_z}{\partial z} = 0, \tag{25}$$

where λ_{11} and λ_{33} are dielectric constants, D_x, D_z, e_{31}, and ψ show the electric displacements, piezoelectric coefficient, and the electric potential, respectively. E_x and E_z represent the components of the electric field. For the considered nanowire resonator, we suppose that the electrical potential ψ varies between $-h$ to h across the height of the nanowire. Accordingly, we can consider a uniform piezoelectric distribution along the NW. It implies that $\psi_x \ll \psi_z$, therefore, we can neglect the electric displacement D_x in comparison with D_z. Based on this assumption, Eq. (25) will be written in the following form:

$$\frac{\partial D_z}{\partial z} = 0. \tag{26}$$

We consider the following boundary conditions for the electrical potential distribution to solve the above differential equation and combine the term related to the piezoelectric effect with the boundary conditions for the vibrations of the nanowire:

$$\psi(x,-h) = 0, \qquad \psi(x,h) = 2V_e. \tag{27}$$

Using Eqs. (11), (23), (24) and Eq. (26) and assuming the above boundary conditions results in the following form of electrical potential (derivation is provided in Appendix B) :

$$\psi(x,z) = -\frac{e_{31}}{\lambda_{33}}\left(\frac{z^2-h^2}{2}\right)\frac{\partial^2 w}{\partial x^2} + \left(1+\frac{z}{h}\right)V_e, \tag{28}$$

where V_e is the electric voltage [39]. The exerted axial load by piezoelectric potential is obtained using the following equation:

$$p_e = b\int_{-h}^{h} \sigma_{xx} dz. \tag{29}$$

Substituting Eqs. (23) and (28) into Eq. (11), and then into Eq. (29) results in the following form of the axial load:

$$p_e = 2V_e b e_{31}. \tag{30}$$

Combining Eq. (29), Eq. (18) and (21), the following equation is obtained for the axial load, N, indicated in Eq. (31):

$$N = P_e + \frac{EA_{eff}}{2L}\int_0^L \left(\frac{\partial w}{\partial x}\right)^2 dx - \frac{1}{1-2v}\alpha_x\theta_t + 2b\tau_0. \tag{31}$$

Turning to Fig. 1(a) and using the Newton's law, we can write the following formulation for the shear force applied to the nanowire:

$$\frac{\partial V}{\partial x} = (\rho A)_{eff}\frac{\partial^2 w(x,t)}{\partial t^2} + m_p\delta(x-x_p)\frac{\partial^2 w(x,t)}{\partial t^2} + \mu\frac{\partial w(x,t)}{\partial t} + k_1 w(x,t) + k_3 w^3(x,t) - F(x,t) - f_{em}, \tag{32}$$

where ρ, V, μ, m_p, x_p, k_1 and k_3 are density, shear force, damping coefficient, particle mass, position of applied force, linear and nonlinear Winkler coefficient, respectively. The terms $k_1 w(x,t)$ and $k_3 w^3(x,t)$ are the forces exerted to the nanowire resonator by the assumed linear and nonlinear foundations, respectively. The term $k_3 w^3$ is a nonlinear part of Eq. (32).

Substituting Eqs. (31) and (32) into Eq. (3), and then using Eq. (7), results in the following governing equation for the vibrations of piezoelectric nanowire considering an added mass:

$$(EI)_{eff}\frac{\partial^4 w}{\partial x^4} + \left(1 - \Gamma\frac{\partial^2}{\partial x^2}\right)\Psi = 0, \tag{33}$$

where

$$\Psi = (\rho A)_{eff}\frac{\partial^2 w(x,t)}{\partial t^2} + m_p\delta(x-x_p)\frac{\partial^2 w(x,t)}{\partial t^2} + \mu\frac{\partial w(x,t)}{\partial t} + k_1 w(x,t) - 2b\tau_0\frac{\partial^2 w}{\partial x^2} + k_3 w^3(x,t) - F(x,t) - \zeta_m A H_x^2\frac{\partial^2 w}{\partial x^2} + 2V_e b e_{31}\frac{\partial^2 w}{\partial x^2} - \left(\frac{(EA)_{eff}}{2L}\int_0^L\left(\frac{\partial w}{\partial x}\right)^2 dx - N_\theta\right)\frac{\partial^2 w}{\partial x^2}, \tag{34}$$

where the mathematical definition of the parameters used in the above equation can be found in Appendix C [42]. In the above equation, $k_3 w^3$ and $\frac{(EA)_{eff}}{2L}\int_0^L(\frac{\partial w}{\partial x})^2 dx\frac{\partial^2 w}{\partial x^2}$ are nonlinear terms. We need to develop the dimensionless form of the above equation by defining the following variables: $\xi = \frac{x}{L}$, $\bar{W} = \frac{w}{L}$, $\tau = \omega_n t$. Considering these new variables, Eqs. (33) and (34) are rewritten as follows:

$$\frac{\partial^4 \bar{W}}{\partial \xi^4} + \Pi\frac{\partial^2 \bar{W}}{\partial \tau^2} - \Upsilon\Pi\frac{\partial^4 \bar{W}}{\partial \tau^2 \partial \xi^2} + \kappa\frac{\partial^2 \bar{W}}{\partial \tau^2} - \Upsilon\kappa\frac{\partial^4 \bar{W}}{\partial \tau^2 \partial \xi^2} + \Delta\frac{\partial \bar{W}}{\partial \tau} - \Delta\Upsilon\frac{\partial^3 \bar{W}}{\partial \tau \partial \xi^2} + \psi\bar{W} - \psi\Upsilon\frac{\partial^2 \bar{W}}{\partial \xi^2} - 2\frac{\tau_0}{L}\frac{\partial^2 \bar{W}}{\partial \xi^2} + 2\Upsilon\frac{\tau_0}{L^2}\frac{\partial^4 \bar{W}}{\partial \xi^4} - F\left(\frac{\xi}{L},\frac{\tau}{\omega_n}\right) + \Upsilon\frac{\partial^2}{\partial \xi^2}F\left(\frac{\xi}{L},\frac{\tau}{\omega_n}\right) - \Lambda\frac{\partial^2 \bar{W}}{\partial \xi^2} + \Upsilon\Lambda\frac{\partial^4 \bar{W}}{\partial \xi^4} - \gamma_1\frac{\partial^2 \bar{W}}{\partial \xi^2} + \Upsilon\gamma_1\frac{\partial^4 \bar{W}}{\partial \xi^4} + \psi_1\bar{W}^3 + \Upsilon\frac{\partial^2}{\partial \xi^2}\psi_1\bar{W}^3 - \psi_2\left(\int_0^1\left(\frac{\partial \bar{W}}{\partial \xi}\right)^2 d\xi + N_\theta\right)\frac{\partial^2 \bar{W}}{\partial \xi^2} + \psi_2\Upsilon\frac{\partial^2}{\partial \xi^2}\left(\int_0^1\left(\frac{\partial \bar{W}}{\partial \xi}\right)^2 d\xi + N_\theta\right)\frac{\partial^2 \bar{W}}{\partial \xi^2} = 0, \tag{35}$$

where

$$\Upsilon = \left(\frac{e_0 a}{L}\right)^2, \quad \Pi = \frac{L(\rho A)_{eff}\omega_n^2}{\Lambda_1}, \quad \Lambda_1 = \frac{(EI)_{eff}}{L^3}, \quad \Delta = \frac{\mu L\omega_n}{\Lambda_1},$$

$$\kappa = \frac{m_p\delta(1-\frac{x_p}{L})\omega_n^2 L}{\Lambda_1}, \quad \psi = \frac{K_1 L}{\Lambda_1}, \quad \psi_2 = \frac{(EA)_{eff}}{\Lambda_1 L^3},$$

$$\Lambda = \frac{\xi A H_x^2}{L\Lambda_1}, \quad \gamma_1 = \frac{2Vbe_{31}}{L\Lambda_1}.$$

The obtained governing equation of the nanowire resonator will be analyzed using perturbation techniques in the next section taking into account a general form of the boundary conditions.

In order to analyze the oscillations of nanowire resonators and obtain the primary resonance using MMS, the first step is to apply the Galerkin method [44], which discretizes the time dependent part of Eq. (35). Accordingly, we consider the following form for $\bar{W}(\xi,\tau)$ in order to discretize Eq. (35) taking into account the primary mode of nanowire oscillations [44]:

$$\bar{W}(\xi,\tau) = \phi(\xi)\bar{u}(\tau), \tag{36}$$

where $\phi(\xi)$ defines the dimensionless deflection shape of the beam based on the assumed boundary conditions. In Eq. (36), $\bar{u}(\tau)$ represents the dimensionless time dependent part of the oscillations of nanowires. Since our focus is on the vibration and frequency analysis of nanowire resonators, we use the separation of variables to find the time dependent part of the developed model [44]. Using the Galerkin method, we substitute Eq. (36) into Eq. (35) and then taking the integral from both sides of the equation, the following nonlinear ordinary differential equation is obtained:

$$\ddot{\bar{u}} + \frac{\alpha_1}{\alpha_0}\dot{\bar{u}} + \frac{\alpha_2}{\alpha_0}\bar{u} + \frac{\alpha_3}{\alpha_0}\bar{u}^3 = \frac{\alpha_F}{\alpha_0}cos\left(\frac{\Omega}{\omega_n}\tau\right), \tag{37}$$

where details on α_0, α_1, α_2, α_3, and α_F can be found in Appendix D. In order to analyze the Eq. (37), the Method of Multiple Scales [45] will be employed in the next section. The main aim of using MMS is to find the primary and other types of resonances of nanowire vibrations, and then to investigate the effect of different parameters on such vibrations.

3. Implementation of MMS for nanowire resonators

In this section, we illustrate our method on the solution of Eq. (37) for finding primary and super-harmonic resonance cases.

3.1. Primary resonance

In order to solve Eq. (37), we first rewrite it with implementation of small parameter ϵ. Accordingly, we have the following nonlinear

differential equation [46]:

$$\ddot{\bar{u}} + 2\epsilon\bar{\mu}\dot{\bar{u}} + \omega_l^2\bar{u} + \epsilon\bar{\beta}\bar{u}^3 = \epsilon f cos(\Omega_1\tau), \tag{38}$$

where $2\bar{\mu} = \frac{\alpha_1}{\alpha_0}$, $\omega_l^2 = \frac{\alpha_2}{\alpha_0}$, $\bar{\beta} = \frac{\alpha_3}{\alpha_0}$, $f = \frac{\alpha_F}{\alpha_0}$, and $\Omega_1 = \frac{\Omega}{\omega_n}$. For the primary resonance case analysis of the nanowire resonator, modeled in Section 2, the frequency of external excitation Ω_1 should be approximately equal to that of natural frequency ω_l of the nanowire. Hence, to delineate the nearness of Ω_1 to ω_l, one may use a detuning parameter σ, and by using the dimensionless small parameter (ϵ) it can be written as:

$$\Omega_1 = \omega_l + \epsilon\sigma. \tag{39}$$

Now, we can expand $\bar{u}$ as the following equation:

$$\bar{u}(\tau,\epsilon) = \bar{u}_0(T_0,T_1) + \epsilon\bar{u}_1(T_0,T_1). \tag{40}$$

Accordingly, by substituting Eq. (40) into Eq. (38), and then by separating the similar power of ϵ, will result in the following set of differential equations:

$$D_0^2\bar{u}_0 + \omega_l\bar{u}_0 = 0, \tag{41}$$

$$D_0^2\bar{u}_1 + \omega_l\bar{u}_1 = -2D_0D_1\bar{u}_0 - 2\bar{\mu}\bar{u}_0 - \bar{\beta}\bar{u}_0^3 + f\cos(\omega_lT_0 + \sigma T_1). \tag{42}$$

The solution of Eq. (41) can be considered as:

$$u_0 = A(T_1,T_2)\exp(i\omega_lT_0) + \bar{A}(T_1,T_2)\exp(-i\omega_lT_0). \tag{43}$$

By substituting Eq. (43) into Eq. (42), we obtain the following form of equation:

$$D_0^2\bar{u}_1 + \omega_l\bar{u}_1 = -[2i\omega_l(A' + \bar{\mu}A) + 3\bar{\beta}A^2\bar{A}]\exp(i\omega_lT_0) \tag{44}$$
$$-\bar{\beta}A^3\exp(3i\omega_lT_0) + \frac{1}{2}f\exp[i(\omega_lT_0 + \sigma T_1)] + c.c.\ ,$$

where $c.c.$ stands for the complex conjugate terms. The term which contains $\exp(i\omega_lT_0)$ is the secular term. In order to have a bounded solution, the secular terms should be neglected as presented below [47]:

$$2i\omega_l(A' + \bar{\mu}A) + 3\bar{\beta}A^2\bar{A} - \frac{1}{2}f\exp(i\sigma T_1) = 0. \tag{45}$$

Exerting $A = \frac{a}{2}\exp(iB)$ into Eq. (45) and separating the real and imaginary parts, we obtain the following set of ordinary differential equations:

$$a' = -\bar{\mu}a + \frac{1}{2}\frac{f}{\omega_l}\sin(\sigma T_1 - B), \tag{46}$$

$$aB' = \frac{3}{8}\frac{\bar{\beta}}{\omega_l}a^3 - \frac{1}{2}\frac{f}{\omega_l}\cos(\sigma T_1 - B). \tag{47}$$

By defining $\bar{\lambda} = \sigma T_1 - B$, Eqs. (46) and (47) are rewritten as below:

$$a' = -\bar{\mu}a + \frac{1}{2}\frac{f}{\omega_l}\sin(\bar{\lambda}), \tag{48}$$

$$a\bar{\lambda}' = a\sigma + \frac{3}{8}\frac{\bar{\beta}}{\omega_l}a^3 - \frac{1}{2}\frac{f}{\omega_l}\cos(\bar{\lambda}). \tag{49}$$

We can find a steady state solution of the system of Eqs. (48)–(49) by equating a' and $\bar{\lambda}'$ to zero. We know that the amplitude and phase of the system do not depend on the time and hence the time derivative terms of both terms are equal to zero. Therefore, we can have the following equations:

$$\bar{\mu}a = \frac{1}{2}\frac{f}{\omega_l}\sin(\bar{\lambda}), \tag{50}$$

and

$$a\sigma - \frac{3}{8}\frac{\bar{\beta}}{\omega_l}a^3 = \frac{1}{2}\frac{f}{\omega_l}\cos(\bar{\lambda}). \tag{51}$$

Squaring and adding the above equations, the following closed-form relationship is obtained [46]:

$$\left[\bar{\mu}^2 + \left(\sigma - \frac{3}{8}\frac{\bar{\beta}}{\omega_l}a^2\right)^2\right]a^2 = \frac{f^2}{4\omega_l^2}. \tag{52}$$

The above equation is 6th order polynomial in terms of a. It is also a quadratic equation in terms of σ. Solving the above equation for σ, we obtain the following form as the frequency response curve for the Eq. (38):

$$\sigma = \frac{3}{8}\frac{\bar{\beta}}{\omega_l}a^2 \pm \left[\frac{f^2}{4\omega_l^2} - \bar{\mu}^2\right]^{\frac{1}{2}}. \tag{53}$$

The obtained relationship will be used in the next sections to quantify the effect of different parameters on the primary resonance of the nanowire resonator.

3.2. Super-harmonic resonance

The other resonance case that can be used for the sensitivity analysis of the considered nanowire resonators is the super-harmonic resonance case. The super-harmonic case occurs when $\Omega_1 \simeq \frac{1}{3}\omega_l$ [45]. This resonance case can also be considered for finding the effect of the added mass on the frequency behavior of nanowire resonators. In order to assess this case, following [45], we define the super-harmonic resonance case as:

$$3\Omega_1 = \omega_l + \epsilon\sigma. \tag{54}$$

We assume the solution of Eq. (37) in the following form [45]:

$$\bar{u}_0 = A(T_1)\exp(i\omega_lT_0) + \bar{\Gamma}\exp(i\Omega_1T_0) + c.c. \tag{55}$$

Substituting Eq. (55) into Eq. (37) results in:

$$D_0^2\bar{u}_1 + \omega_l\bar{u}_1 = -[2i\omega_l(A' + \bar{\mu}A) + 3\bar{\beta}A^2\bar{A} + 6\bar{\beta}A\bar{\Gamma}^2]\exp(i\omega_lT_0) \tag{56}$$
$$-\bar{\beta}[A^3\exp(3i\omega_lT_0)] + \bar{\Gamma}^3\exp(3i\Omega_1T_0) + 3A^2\bar{\Gamma}\exp[i(2\omega_l + \Omega_1)T_0]$$
$$+3\bar{A}^2\bar{\Gamma}\exp[i(\Omega_1 - 2\omega_l)T_0] + 3A\bar{\Gamma}^2\exp[i(\omega_l + 2\Omega_1)T_0] +$$
$$3\bar{A}\bar{\Gamma}^2\exp[i(\omega_l - 2\Omega_1)T_0]] - \bar{\Gamma}[2i\bar{\mu}\Omega_1 + 3\bar{\beta}\bar{\Gamma}^2 + 6\alpha A\bar{A}]\exp(i\Omega_1T_0) + c.c.,$$

where

$$\bar{\Gamma} = \frac{f}{2\times(\omega_l^2 - \Omega_1^2)}. \tag{57}$$

For this resonance case, we must follow the resonance condition as below [45]:

$$3\Omega_1T_0 = (\omega_l + \epsilon\sigma)T_0 = \omega_lT_0 + \epsilon\sigma T_0. \tag{58}$$

Now, we can eliminate the secular and near secular terms in Eq. (56) which leads to following equation:

$$2i\omega_l(A' + \bar{\mu}A) + 6\bar{\beta}\bar{\Gamma}^2A + 3\bar{\beta}A^2\bar{A} + \bar{\beta}\bar{\Gamma}^3\exp(i\sigma T_1) = 0. \tag{59}$$

Using $A = \frac{a}{2}\exp(iB)$ and separating the real and imaginary parts, we obtain:

$$a' = -\bar{\mu}a - \frac{\alpha\bar{\Gamma}^3}{\omega_l}\sin(\sigma T_1 - B), \tag{60}$$

$$aB' = \frac{3\bar{\beta}}{\omega_l}\left(\bar{\Gamma}^2 + \frac{1}{8}a^2\right)a - \frac{\bar{\beta}\bar{\Gamma}^3}{\omega_l}\cos(\sigma T_1 - B). \tag{61}$$

Using the defined $\bar{\lambda}$ for the primary resonance case, we obtain the following equations:

$$a' = -\bar{\mu}a - \frac{\alpha\bar{\Gamma}^3}{\omega_l}sin(\bar{\lambda}), \tag{62}$$

$$a\bar{\lambda}' = \left(\sigma - \frac{3\bar{\beta}\bar{\Gamma}^2}{\omega_l}\right)a - \frac{3\bar{\beta}}{8\omega_l}a^3 - \frac{\bar{\beta}\bar{\Gamma}^3}{\omega_l}\cos(\bar{\lambda}). \tag{63}$$

We can find a steady state solution of Eqs. (62)–(63) by equating a' and $\bar{\lambda}'$ to zero. Accordingly, the following set of equations is obtained:

$$\bar{\mu}a = -\frac{\alpha\bar{\Gamma}^3}{\omega_l}\sin(\bar{\lambda}), \tag{64}$$

$$\left(\sigma - \frac{3\bar{\beta}\bar{\Gamma}^2}{\omega_l}\right)a = \frac{3\bar{\beta}}{8\omega_l}a^3 + \frac{\bar{\beta}\bar{\Gamma}^3}{\omega_l}\cos(\bar{\lambda}). \tag{65}$$

Eliminating $\bar{\lambda}$ in the above equations, the following closed form relation can be obtained:

$$\left[\bar{\mu}^2 + \left(\sigma - 3\frac{\bar{\beta}\bar{\Gamma}^2}{\omega_l} - \frac{3\bar{\beta}}{8\omega_l}a^2\right)^2\right]a^2 = \frac{\bar{\beta}^2\bar{\Gamma}^6}{\omega_l^2}. \tag{66}$$

Solving the above equation based on the detuning parameter (σ) and amplitude of oscillations (a), we obtain the following closed form relationship for the super-harmonic resonance case:

$$\sigma = 3\frac{\bar{\beta}\bar{\Gamma}^2}{\omega_l} + \frac{3\bar{\beta}}{8\omega_l}a^2 \pm \sqrt{\frac{\bar{\beta}^2\bar{\Gamma}^6}{\omega_l^2 a^2} - \bar{\mu}^2}. \tag{67}$$

Following [45], the maximum amplitude for the case of super-harmonic resonance can be found using the following formula:

$$a_p = \frac{\bar{\beta}\bar{\Gamma}^3}{\bar{\mu}\omega_l}. \tag{68}$$

Therefore, the super-harmonic resonance in the case of maximum amplitude of oscillation is given as follows [45]:

$$\sigma_p = \frac{3\bar{\beta}\bar{\Gamma}^2}{\omega_l}\left[1 + \frac{\bar{\beta}\bar{\Gamma}^4}{8\bar{\mu}^2\omega_l^2}\right]. \tag{69}$$

4. Online parameter identification technique (OPIT)

In what follows, we treat the added mass m_p as an unknown parameter of Eq. (37). Based on Eq. (37), we know that m_p is defined by α_0. Therefore, for the identification of m_p, we should first obtain α_0. Using Eq. (37), a linear parametric model is developed to estimate α_0. It should be noted that we assume that u is the only available measurable signal. In order to generate stable signal of $\dot{u}$ and ü, we apply the stable filters of $\frac{s}{\Delta(s)}$ and $\frac{s^2}{\Delta(s)}$ to signal u. With applying the considered low pass filter, the following linear parametric model is obtained [48]:

$$q_0 = \alpha_0\phi_0, \tag{70}$$

where

$$q_0 = \frac{1}{\Delta(s)}z - \alpha_1\frac{1}{\Delta(s)}u - \alpha_2\frac{s}{\Delta(s)}u - \alpha_3\frac{s}{\Delta(s)}u^3, \tag{71}$$

in which q_0, ϕ, $\Delta(s)$, and z are respectively, the measurable model output signal, regressor signal, stable second order polynomial, and external force defined in Eq. (37). In accordance with the developed linear parametric model, an on-line gradient-based parameter estimator is proposed to estimate the actual value of α_0 as follows:

$$q_0 = \hat{\alpha}_0\phi_0, \tag{72}$$

$$\epsilon_0 = \frac{\alpha_0 - \hat{\alpha}_0}{m_{s_0}^2}, m_{s_0}^2 = 1 + k_{s_0}\phi_0^2, k_{s_0} > 0, \tag{73}$$

in which $\hat{\alpha}_0$ characterizes the online estimated value of α_0 and ϵ_0 is the estimation error. Based on the adaptive gradient law and the developed identification method, we show that with the use of Eq. (37) and measuring the displacement of nanowire, we can estimate the added mass to it. In Section 5.3, we demonstrate the capability of the proposed method for identifying tiny masses.

5. Sensitivity analysis

In this section, we investigate the effect of different parameters on the behavior of nanowire resonator with added mass considering both linear and nonlinear vibrations in two different sections.

5.1. Linear case

This section provides a sensitivity analysis of the effect of different parameters on the vibration frequency of the nanowire resonator with simply supported boundary conditions in which $\bar{W}(0,\tau) = 0$, $\frac{\partial^2\bar{W}}{\partial\xi^2}(0,\tau) = 0$ at left end, and $\bar{W}(1,\tau) = 0$, $\frac{\partial^2\bar{W}}{\partial\xi^2}(1,\tau) = 0$ at the right end of the beam. The shape function of the first mode is assumed as $\phi(\xi) = \sin(\pi\xi)$. Based on Ref. [49], we consider the following sizes for the nanowire: $h = 1$ nm, $b = 3$ nm and $L = 15$ nm. In addition, the properties of silicon nanowire was used for the simulations. Regarding the material of our nanoresonator, we use the properties of silicon nanowire Figures of this section have been plotted based on the dimensionless linear frequency of the nanowire resonator with respect to dimensionless added mass. The dimensionless linear frequency is defined by the following equation:

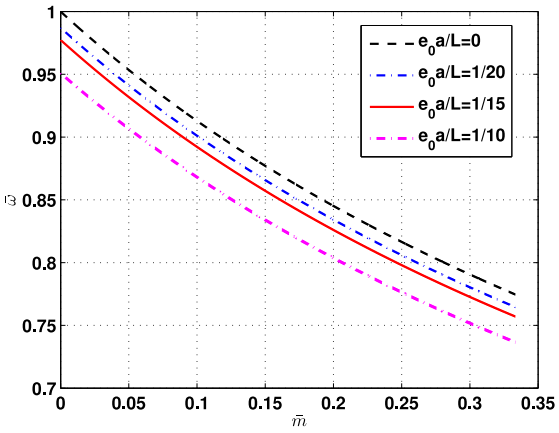

Fig. 2. (Color online) Effect of the nonlocal parameter and added mass on the linear frequency of the SiNW.

$$\bar{\omega} = \frac{\omega_l}{\omega_0}, \tag{74}$$

where ω_0 is the linear frequency of the nanowire resonator without added mass and it can be obtained by using Eqs. (D.1) and (D.3). The dimensionless mass $\bar{m}$ is defined as below:

$$\bar{m} = \frac{m_p}{m_{nw}}, \tag{75}$$

where m_p and m_{nw} represent the masses of the added particle and the nanowire, respectively. Fig. 2 shows the effect of dimensionless nonlocal parameter ($\frac{e_0a}{L}$) and added mass ($\bar{m}$) on the dimensionless linear frequency. As the figure demonstrates, increasing the added mass results in decreasing the frequency. In addition, the value of frequency decreases by increasing the nonlocal parameter for a given added mass. Fig. 3 represents the effect of temperature on the linear frequency of the nanowire. Based on this figure, increasing temperature results in decreasing the linear natural frequency for a given added mass. Although temperature variations result in a small shift in the frequency of the nanowire for a specific added mass, it may affect the sensitivity of the nanowire resonator for small mass sensing such as bio-objects, significantly.

The effect of piezoelectric voltage is presented in Fig. 4. As displayed by this figure, increasing the piezoelectric voltage decreases the frequency of oscillations of nanowire resonator. In addition, it shows that the piezoelectric voltage has a more pronounced effect on the vibration behavior of the nanowire resonator in comparison with thermal variations. This figure shows that the piezoelectric voltage significantly changes the sensitivity of the nanowire resonator. Accordingly, the frequency of the nanowire resonator can be adjusted by using a specific piezoelectric voltage. The effect of magnetic field is presented in Fig. 5. This figure shows that the magnetic field can be used for increasing the natural frequency of the nanowire. Therefore, it can be utilized as a design parameter to adjust the frequency of the nanowire to a specific value required for a mass sensing application. It must be noted that the effect of electromagnetic fields on the vibrations of

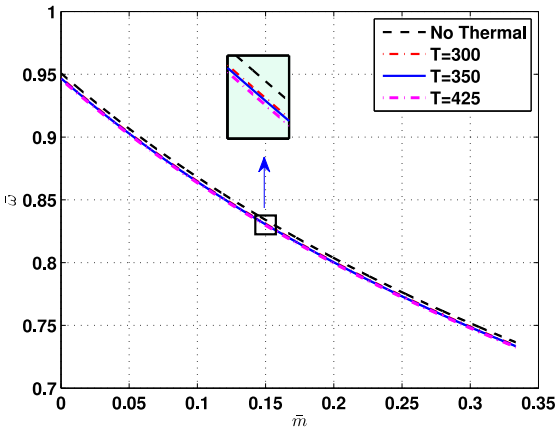

Fig. 3. (Color online) Effect of the temperature $[^oK]$ variations and added mass on the linear frequency of SiNW.

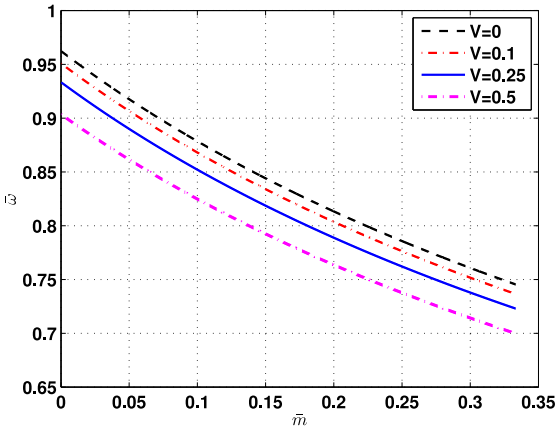

Fig. 4. (Color online) Effect of the piezoelectric voltage [V] and added mass on the linear frequency of SiNW.

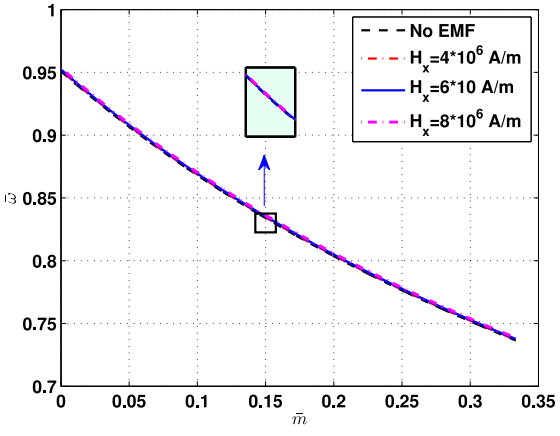

Fig. 5. (Color online) Effect of the magnetic field and added mass on the linear frequency of SiNW.

resonators is not very big but it is considerable for sensing applications with high precision. All of these figures show that adding a tiny mass to a nanowire would result in a detectable frequency shift. This frequency shift can be measured and used for detection of the added mass in the case of experimental analysis.

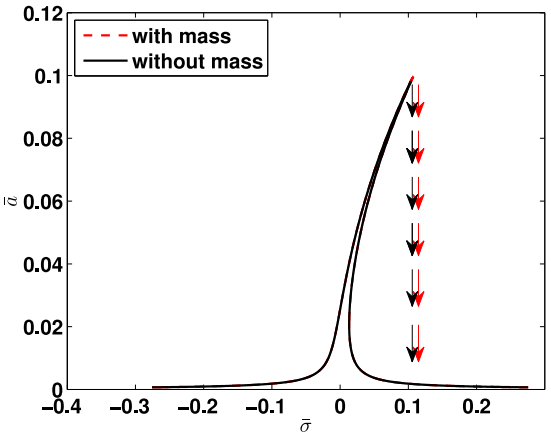

Fig. 6. (Color online) Effect of the added mass on the primary resonance of SiNW.

5.2. Nonlinear vibration

In this part, we study nonlinear vibrations of the nanowire using the obtained primary resonance in Section 3, accounting for simply supported boundary conditions.

5.2.1. Primary resonance

Based on Eq. (53) developed in Section 3, we investigate the effect of added mass on the primary resonance of nanowire resonators. Fig. 6 represents the effect of the added mass on the primary resonance of nanowire resonators. As the figure shows, adding a small mass (e.g., $m_p = 10^{-18}g$) to the nanowire results in a detectable shift in the jump frequency. This jump can be observed in the experimental analysis [1]. This observation can be analyzed using the model developed in this paper. It should be noted ultra-high mass sensing experiments are generally performed in vacuum conditions to either alleviate or avoid potential noises. Therefore, we can have the capability of parametric sensitivity analysis of nanowire resonators both mathematically and experimentally [50]. In addition, Fig. 6 demonstrates a high sensitivity of the nanowire resonator to a very small mass. It affects both the jump frequency and also amplitude of oscillations. Accordingly, it can be concluded that nanowire resonators have a high potential for detection of tiny particles such as bio-objects.

Fig. 7 shows the effect of thermal variations on the primary resonance of the nanowire resonator. As the figure presents, increasing temperature results in increasing the amplitude of oscillations. In fact, increasing temperature reduces the stiffness of the resonator, and therefore, both amplitude of oscillations and the value of jump frequency increase. Temperature fluctuation can limit the Q-factor of nanoresonators and accordingly their sensing performance [51]. Studying the temperature effect, as pictured in Fig. 7, results in having a better control over the frequency behavior of nanowire resonators. This analysis can help in designing feedback cooling with the aim of mitigation of frequency fluctuations owing to temperature variations. Analogous results can be obtained when the piezoelectric voltage increases (see Fig. 8). Increasing the piezoelectric voltage results in increasing the amplitude of oscillations and also the value of the jump frequency. Accordingly, these two parameters can be used for adjusting the amplitude and the jump frequency of the nanowire resonator. In many practical situations of sensing, it is important to consider the effect of these two parameters in measurements as they affect both vibration amplitude and also frequency. The effect of electromagnetic fields is presented in Fig. 9 based on the obtained primary resonance in Section 3. As the figure demonstrates, increasing the value of the magnetic field reduces the value of jump frequency of the nanowire resonator. In addition, the value of amplitude of oscillations of the

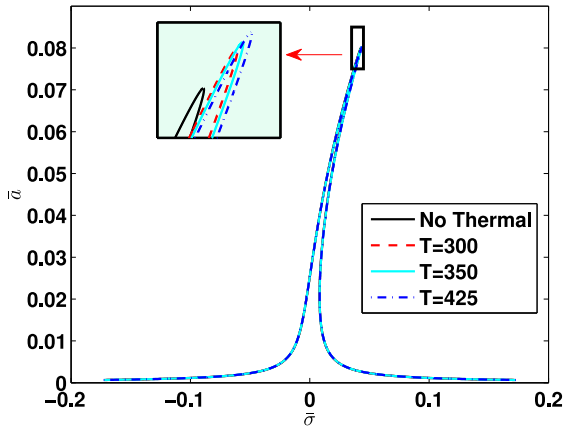

Fig. 7. (Color online) Effect of the temperature $[^{o}K]$ variations on the primary resonance of the SiNW.

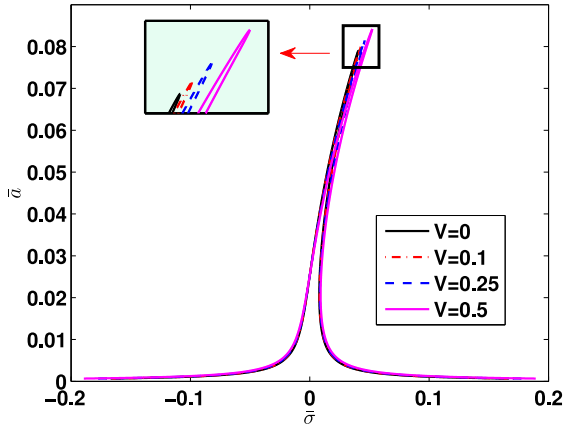

Fig. 8. (Color online)Effect of the piezoelectric voltage $[V]$ on the primary resonance of SiNW.

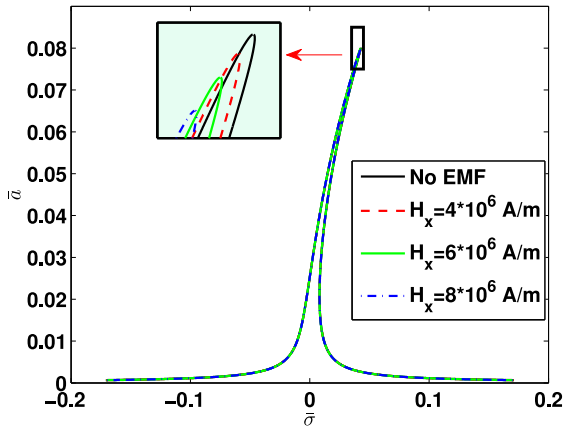

Fig. 9. (Color online) Effect of the magnetic field on the primary resonance of SiNW.

nanowire resonator decreases with increasing the value of the magnetic field.

5.2.2. Super-harmonic resonance

In this section, we focus on the super-harmonic resonance case of our silicon nanowire resonator and the effect of different parameters on the peak amplitude defined by Eq. (68) and its corresponding σ_p obtained in Eq. (69). All figures of this section are obtained based

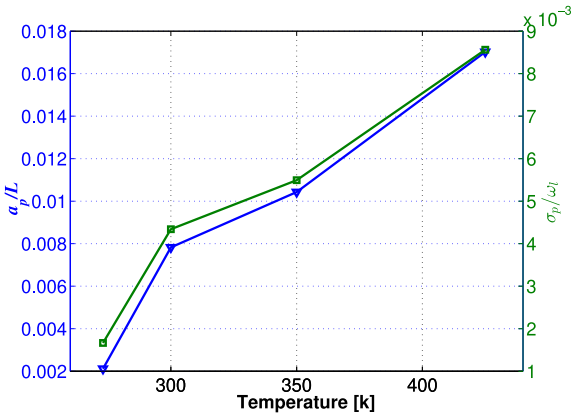

Fig. 10. (Color online) Effect of temperature on the peak amplitude and the detuning parameter of the super-harmonic resonance of SiNW.

on Eq. (68) and (69) with simply supported boundary conditions. In these figures, the blue and green lines are related to the amplitude of oscillations and super-harmonic resonance, respectively. Furthermore, the natural frequency (ω_l) is approximately equal to 66.6 GHz. Fig. 10 shows the effect of temperature variations on both dimensionless peak amplitude (a_p) and its corresponding detuning parameter (σ_p). The corresponding values are obtained for four different temperatures: $T = 273,\ 300,\ 350$, and $450\ ^{\circ}K$ [52]. Based on this figure, the detuning parameter of the super-harmonic resonance, σ_p, is 5.38 GHz at the temperature of $425\ ^{\circ}K$. The corresponding amplitude of oscillations, a_p, is 0.25 nm. As the figure demonstrates, increasing environmental temperature increases both a_p and σ_p. Therefore, not only we can look at the primary resonance to understand the behavior of the nanowire under thermal variations, but also, we can investigate the super-harmonic resonance as an alternative approach for understanding the response of the nanowire resonator under different thermal conditions. As it was expected both primary and super-harmonic resonance cases show similar behaviors under thermal loads.

Fig. 11 reveals the effect of magnetic field on the super-harmonic resonance of nanowire resonators. The figure shows the relation of both a_p and σ_p to the variation of magnetic flux density for the super-harmonic resonance case. Similar to the primary resonance, increasing the magnetic flux density decreases both a_p and σ_p. It should be noted that $\bar{H}_x$ represents the dimensionless form of the magnetic flux density.

Fig. 12 shows the effect of piezoelectric voltage on both a_p and σ_p. As the figure depicts, increasing the piezoelectric voltage enhances both a_p and σ_p of the nanowire resonator.

5.3. Discussion based on OPIT

By using OPIT, it has been shown that the proposed model can be used to find a tiny mass rested on the nanowire resonator. Fig. 13 represents the results of identification technique based on the proposed mathematical model. As the figure demonstrates, we can identify the added mass even on the order of 10^{-21} Kg using the nanowire resonator for a short period of time. In Fig. 13, blue and red lines represent the estimated and actual masses, respectively.

6. Molecular dynamics simulation

In order to investigate the potential of nanowire resonators for the detection of biological objects, we use MD simulations to analyze the frequency response of nanowire resonators after adding an HIV virus as an example. This methodology, which has also been applied recently in the context of RNA nanostructures and other complex biological

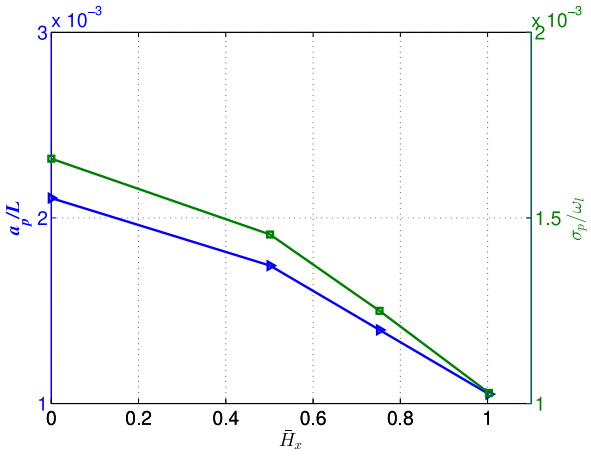

Fig. 11. (Color online) Effect of magnetic field on the peak amplitude and the detuning parameter of the super-harmonic resonance of SiNW.

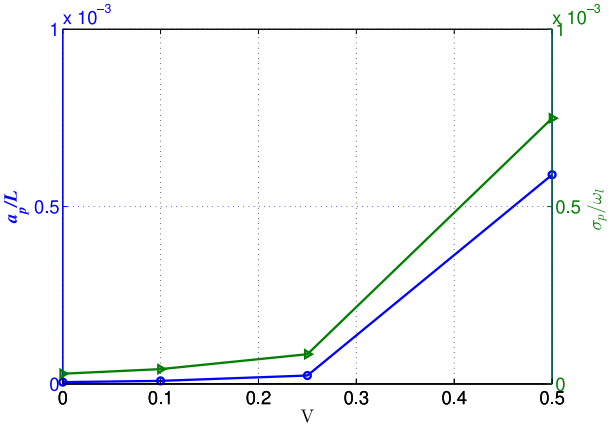

Fig. 12. (Color online) Effect of piezoelectric voltage on the peak amplitude and the super-harmonic resonance of SiNW.

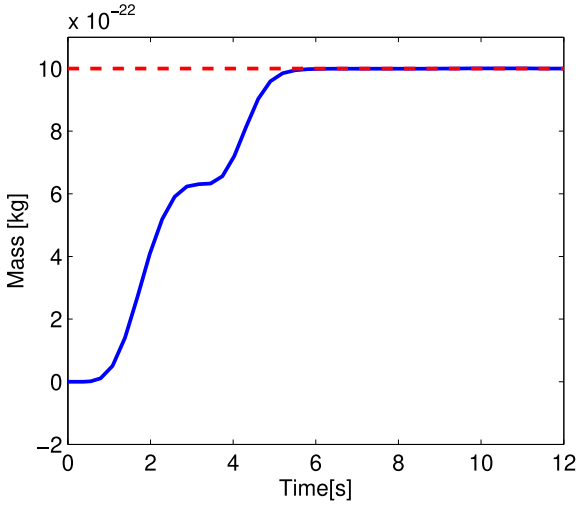

Fig. 13. (Color online) Online Identification of Added Mass.

systems [53–56], is much more computationally time consuming, compared to the methodologies based on continuum models. At the same time, the MD methodology has been used in the development of new

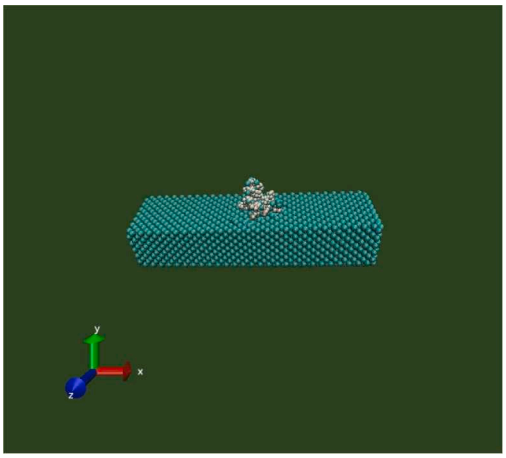

Fig. 14. Nanowire resonator with attached mass (HIV virus) at $T = 300$ °K.

atomistic-to-continuum models for tiny biological structures [57]. Here, we locate an HIV virus in the middle of the nanowire resonator as shown in Fig. 14. We first examine the nanowire resonator without an added HIV molecule and obtain its frequency, for this case, by using MD simulations as 43.63 GHz. After adding the molecule of HIV virus, using the higher amplitude peak as a Ref. [58], it has been concluded that the frequency of SiNW resonator decreases to 21.81 GHz, as presented in Fig. 15(b).

7. Conclusions

In this paper, we presented a novel mathematical model for the vibration of nanowire resonators with an added mass taking into account critical parameters. With the implementation of the Euler–Bernoulli beam theory in conjunction with the Eringen nonlocal theory, a nonlinear model was developed to study the vibrations of nanowire resonators, considering surface and thermal effects, as well as the effects of electromagnetic fields, piezoelectric potential, external load, nonlinear foundation, added mass and large oscillations. The obtained governing equation for the vibrations of nanowire resonators was solved by an analytical technique. In order to obtain an analytical solution for the vibrations of nanowires, the method of multiple scales was used to find primary and super-harmonic resonances of the device. Based on the obtained information, we then investigated the frequency shift due to the tiny added mass to the nanowire resonator. In addition, using the developed primary and super-harmonic resonance cases, the effect of different key parameters, such as thermal variations, electromagnetic fields, and the piezoelectric potential, on the vibration behavior of nanowire resonator was studied. The main concluding remarks based on the presented perturbation analysis and developed model are as follows:

- It is shown that the nanowire resonator is capable of detecting tiny masses even in the order of zeptogram. As the mass of added particle increases, the frequency of nanowire resonator reduces.
- Increasing temperature and piezoelectric voltage reduces the frequency of nanowire resonator. It means that when the nanowire resonator is used for tiny mass sensing applications, temperature and piezoelectric potential should be monitored.
- It is observed that increasing electromagnetic fields enhances the stiffness and also frequency of nanowire resonators. This is also another important factor that should be taken into account for designing nanowire resonators in sensing applications.

One of the directions of future studies can include the molecular dynamics simulations of nanowire resonators taking into account all

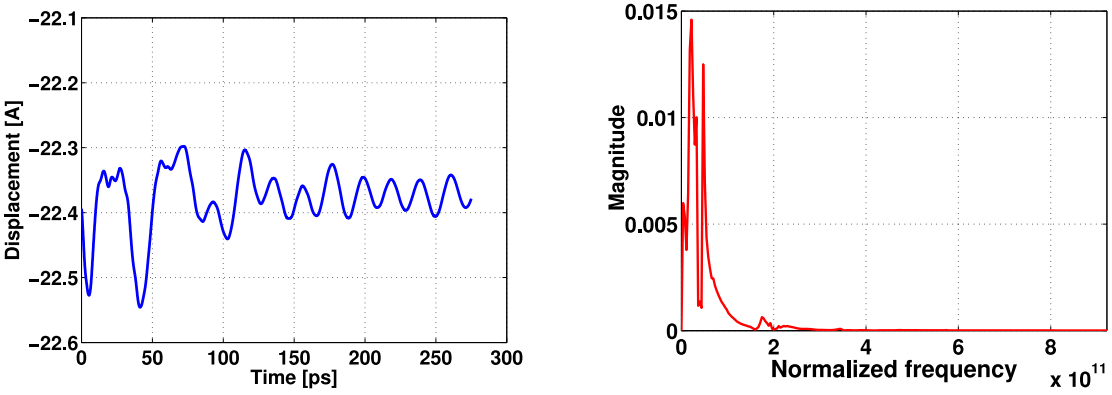

(a) Central atom displacement (b) FFT

Fig. 15. Nanowire resonator with attached mass (HIV virus) at $T = 300$ °K.

effects considered in the developed mathematical model. A complete stability analysis of such nanowire resonators would also present substantial interest for future research. In order to carry out such an analysis, the developed model can be extended by using a time dependent temperature and taking piezoelectric functions into account as $\theta_t = \theta_0 + \theta_1 \cos(\omega_\theta t) p_e = 2(V_{e_0} + V_{e_1} \cos(\omega_p t)) b e_{31}$.

CRediT authorship contribution statement

Rosa Fallahpour: Developed the mathematical model, molecular dynamic simulation, numerical analysis and results, Written and edited the manuscript, Reviewed the final draft, Agreed the latest results and content of the manuscript. **Roderick Melnik:** Written and edited the manuscript, Supervision, Conceptualization, Developing the idea, Reviewed the final draft, Agreed the latest results and content of the manuscript.

Declaration of competing interest

The authors declare that they have no known competing financial interests or personal relationships that could have appeared to influence the work reported in this paper.

Acknowledgments

The authors are grateful to the NSERC, Canada and the CRC, Canada Program for their support. R.M. is also acknowledging the support of the BERC, Spain 2018–2021 program and Spanish Ministry of Science, Innovation, and Universities through the Agencia Estatal de Investigacion (AEI) BCAM Severo Ochoa excellence accreditation SEV-2017-0718, and the Basque Government fund, Spain "AI in BCAM EXP. 2019/00432".

Appendix A. Mathematical procedure for finding the electromagnetic field

To include the electromagnetic field effect into the governing equations of nanowire resonators, based on the Maxwell equations [59,60], we have the following set of equations in the Cartesian coordinates, (x, y, z), as presented in Fig. 1(a):

$$J = \nabla \times h_m, \tag{A.1}$$

$$\nabla \times e_m = \zeta_m \frac{\partial h_m}{\partial t}, \tag{A.2}$$

$$\nabla \cdot h_m = 0, \tag{A.3}$$

$$e_m = -\zeta_m \frac{\partial U}{\partial t} \times H_m, \tag{A.4}$$

$$h_m = \nabla \times (U \times H_m), \tag{A.5}$$

where J, e_m, h_m, U and ζ_m represent current density, strength vectors of electric field, disturbing vectors of magnetic field, the vectors of displacement, and the magnetic permeability, respectively. In order to obtain the magnetic field, which applies the transverse force to the nanowire, we first consider the general case of $U = (u, v, w)$ as the displacement vector. Accordingly, we assume a longitudinal magnetic field vector as $H_m = (H_x, 0, 0)$. Therefore, we obtain:

$$h_m = \nabla \times (U \times H_m) = -H_x \left(\frac{\partial v}{\partial y} + \frac{\partial w}{\partial x} \right) \hat{i} + H_x \frac{\partial v}{\partial x} \hat{j} + H_x \frac{\partial w}{\partial x} \hat{k} \tag{A.6}$$

and

$$J = \nabla \times h_m = H_x \left(\frac{\partial^2 v}{\partial x \partial z} + \frac{\partial^2 v}{\partial x \partial y} \right) \hat{i} - H_x \left(\frac{\partial^2 v}{\partial y \partial z} + \frac{\partial^2 v}{\partial x^2} + \frac{\partial^2 w}{\partial z^2} \right) \hat{j} + H_x \left(\frac{\partial^2 v}{\partial x^2} + \frac{\partial^2 v}{\partial y^2} + \frac{\partial^2 w}{\partial y \partial z} \right) \hat{k}. \tag{A.7}$$

The Lorentz force f_L exerted by the longitudinal magnetic field is obtained by using the following equation [59,60]:

$$f_L = \zeta_m (J \times H_m) = \zeta_m \left[0\hat{i} + H_x^2 \left(\frac{\partial^2 v}{\partial x^2} + \frac{\partial^2 v}{\partial y^2} + \frac{\partial^2 w}{\partial y \partial z} \right) \hat{j} + H_x^2 \left(\frac{\partial^2 w}{\partial x^2} + \frac{\partial^2 w}{\partial y^2} + \frac{\partial^2 v}{\partial y \partial z} \right) \hat{k} \right]. \tag{A.8}$$

Therefore, the components of Lorentz force in x,y, and z directions are defined as follows:

$$f_x = 0, \tag{A.9}$$

$$f_y = \zeta_m H_x^2 \left(\frac{\partial^2 v}{\partial x^2} + \frac{\partial^2 v}{\partial y^2} + \frac{\partial^2 w}{\partial y \partial z} \right), \tag{A.10}$$

$$f_z = \zeta_m H_x^2 \left(\frac{\partial^2 w}{\partial x^2} + \frac{\partial^2 w}{\partial y^2} + \frac{\partial^2 v}{\partial y \partial z} \right). \tag{A.11}$$

We note also that within the developed modeling framework, more refined models for nanowires can potentially be used that account for electronic and enhanced coupled properties [61–64], as well as various types of novel resonators with memory effects can be explored [65,66].

Appendix B. Representation of piezoelectric potential

Substituting Eq. (24) into Eq. (26) yields the following partial differential equation:

$$\frac{\partial (e_{31} \epsilon_{xx})}{\partial z} + \lambda_{33} \frac{\partial E_z}{\partial z} = 0. \tag{B.1}$$

Using Eq. (23) we will have:

$$e_{31} \frac{\partial \epsilon_{xx}}{\partial z} - \lambda_{33} \frac{\partial^2 \psi}{\partial z^2} = 0. \tag{B.2}$$

Implementing Eq. (2) to Eq. (B.2) results in a relationship as follows:

$$e_{31}\left[\frac{\partial}{\partial z}\left(\frac{\partial u}{\partial x}-z\frac{\partial^2 w}{\partial x^2}+\frac{1}{2}(\frac{\partial w}{\partial x})^2\right)\right]-\lambda_{33}\frac{\partial^2\psi}{\partial z^2}=0. \tag{B.3}$$

In Eq. (B.3), the $\frac{\partial u}{\partial x}$ and $\frac{1}{2}(\frac{\partial w}{\partial x})^2$ terms will be omitted. Therefore, this equation (Eq. (B.3)) can be rearranged to take the following form:

$$\frac{\partial^2\psi}{\partial z^2}=-\frac{e_{31}}{\lambda_{33}}\frac{\partial^2 w}{\partial x^2}. \tag{B.4}$$

In order to solve the above-mentioned partial differential equation, we take the integral from both sides of it, which results in the following:

$$\psi(x,z)-\frac{e_{31}}{2\lambda_{33}}z^2\frac{\partial^2 w}{\partial x^2}+C_1 z+C_2, \tag{B.5}$$

where C_1 and C_2 are the constants of integration. For the purpose of obtaining C_1 and C_2, we apply the boundary conditions as provided in Eq. (27). Thus, we will have the following form of equations:

$$-\frac{e_{31}}{2\lambda_{33}}\frac{\partial^2 w}{\partial x^2}(-h)^2+C_1(-h)+C_2=0, \tag{B.6}$$

and

$$-\frac{e_{31}}{2\lambda_{33}}\frac{\partial^2 w}{\partial x^2}(h)^2+C_1(h)+C_2=2V_e. \tag{B.7}$$

Based on Eq. (B.6) we have:

$$C_2=\frac{e_{31}}{2\lambda_{33}}\frac{\partial^2 w}{\partial x^2}h^2+C_1 h. \tag{B.8}$$

By substituting Eq. (B.8) into Eq. (B.7) we obtain the following relationship for C_1:

$$C_1=\frac{V_e}{h}. \tag{B.9}$$

Now, we plug C_1 and C_2, obtained in Eqs. (B.8) and (B.9), in Eq. (B.5) which results in a relationship for the piezoelectric potential as follows:

$$\psi(x,z)=-\frac{e_{31}}{\lambda_{33}}\left(\frac{z^2-h^2}{2}\right)\frac{\partial^2 w}{\partial x^2}+\left(1+\frac{z}{h}\right)v. \tag{B.10}$$

Appendix C. Parameters in Eqs. (33) and (34)

The parameters in Eqs. (33) and (34) are defined as follows:

$$(\rho A)_{eff}=\rho A+2b\rho_0, \tag{C.1}$$

$$(EI)_{eff}=EI+2E^s+4E^s\frac{h^3}{3}-vI\frac{\tau_0}{h}+\frac{2be_{31}^2h^3}{3\lambda_{33}}, \tag{C.2}$$

$$(EA)_{eff}=Ebh+2E^s(b+h), \tag{C.3}$$

$$F(x,t)=\bar{F}\delta(x-x_p)cos(\Omega t), \tag{C.4}$$

$$N_\theta=\frac{1}{1-2v}\alpha_x\theta_t. \tag{C.5}$$

Appendix D. Coefficients of eq. (37)

The coefficients of Eq. (37) can be obtained by the following integrals:

$$\alpha_0=\Pi(\int_0^1\phi^2(\xi)d\xi-\Upsilon\int_0^1\phi''(\xi)\phi(\xi)d\xi)+\kappa(\int_0^1\phi^2(\xi)d\xi-\Upsilon\int_0^1\phi''(\xi)\phi(\xi)d\xi), \tag{D.1}$$

$$\alpha_1=\Delta(\int_0^1\phi^2(\xi)d\xi-\Upsilon\int_0^1\phi^\varepsilon(\xi)\phi(\xi)d\xi), \tag{D.2}$$

$$\alpha_2=\Pi(\int_0^1\phi^2(\xi)d\xi-\Upsilon\int_0^1\phi''(\xi)\phi(\xi)d\xi)-\psi(\int_0^1\phi^2(\xi)d\xi-\Upsilon\int_0^1\phi''(\xi)\phi(\xi)d\xi)+\frac{2\tau_0}{L}(\int_0^1\phi^2(\xi)d\xi-\Upsilon\frac{2\tau_0}{L^2}\int_0^1\phi''(\xi)\phi(\xi)d\xi)-\gamma_1(\int_0^1\phi''(\xi)\phi(\xi)d\xi-\Upsilon\int_0^1\phi''''(\xi)\phi(\xi)d\xi)\Lambda(\int_0^1\phi''(\xi)\phi(\xi)d\xi-\Upsilon\int_0^1\phi''''(\xi)\phi(\xi)d\xi)-\psi_2\frac{1}{1-2\nu}\alpha_x\theta_t(\int_0^1\phi''(\xi)\phi(\xi)d\xi)-\Upsilon(\int_0^1\phi''''(\xi)\phi(\xi)d\xi), \tag{D.3}$$

$$\alpha_3=-\psi_2\int_0^1\phi'(\xi)^2\phi''(\xi)\phi(\xi)d\xi+\Upsilon\frac{\partial^2}{\partial^2\xi}(\psi_2\int_0^1\phi'(\xi)^2\phi'(\xi)\phi(\xi)d\xi), \tag{D.4}$$

and

$$\alpha_F=\bar{F}\left[\int_0^1\delta\left(1-\frac{x_p}{L}\right)\phi(\xi)d\xi-\Upsilon\frac{\partial^2}{\partial\xi^2}\int_0^1\delta\left(1-\frac{x_p}{L}\right)\phi(\xi)d\xi\right], \tag{D.5}$$

where δ is the Dirac function.

References

[1] H. Cho, M. Yu, A. Vakakis, L. Bergman, D. McFarland, Tunable, broadband nonlinear nanomechanical resonator, Nano Lett. 10 (5) (2010) 1793–1798.
[2] E. Asadi, H. Askari, M. Khamesee, A. Khajepour, High frequency nano electromagnetic self-powered sensor: Concept, modelling and analysis, Measurement 107 (2017) 31–40.
[3] G. Gruber, C. Urgell, A. Tavernarakis, A. Stavrinadis, S. Tepsic, C. Magen, S. Sangiao, J.M. De Teresa, P. Verlot, A. Bachtold, Mass sensing for the advanced fabrication of nanomechanical resonators, Nano Lett. 19 (10) (2019) 6987–6992.
[4] K. Eom, H.S. Park, D. Yoon, T. Kwon, Nanomechanical resonators and their applications in biological/chemical detection: nanomechanics principles, Phys. Rep. 503 (4–5) (2011) 115–163.
[5] D. Ramos, M. Arroyo-Hernandez, E. Gil-Santos, H. Tong, C. Van Rijn, M. Calleja, J. Tamayo, Arrays of dual nanomechanical resonators for selective biological detection, Anal. Chem. 81 (6) (2009) 2274–2279.
[6] M. Dilena, M.F. Dell'Oste, J. Fernández-Sáez, A. Morassi, R. Zaera, Mass detection in nanobeams from bending resonant frequency shifts, Mech. Syst. Signal Process. 116 (2019) 261–276.
[7] Q. Wan, Q. Li, Y. Chen, T. Wang, X. He, J. Li, C. Lin, Fabrication and ethanol sensing characteristics of ZnO nanowire gas sensors, Appl. Phys. Lett. 84 (18) (2004) 3654–3656.
[8] M. Eltaher, A. Alshorbagy, F. Mahmoud, Vibration analysis of Euler–Bernoulli nanobeams by using finite element method, Appl. Math. Model. 37 (7) (2013) 4787–4797.
[9] H. Roostai, M. Haghpanahi, Vibration of nanobeams of different boundary conditions with multiple cracks based on nonlocal elasticity theory, Appl. Math. Model. 38 (3) (2014) 1159–1169.
[10] J. Zhou, Z. Wang, A. Grots, X. He, Electric field drives the nonlinear resonance of a piezoelectric nanowire, Solid State Commun. 144 (3–4) (2007) 118–123.
[11] G. Su, Y. Li, X. Li, R. Müllle, Free and forced vibrations of nanowires on elastic substrates, Int. J. Mech. Sci. 138-139 (2018) 62–73.
[12] G. Wang, X. Feng, Effect of surface stresses on the vibration and buckling of piezoelectric nanowires, Europhys. Lett. 91 (5) (2010) 56007.
[13] J. He, C. Lilley, Surface stress effect on bending resonance of nanowires with different boundary conditions, Appl. Phys. Lett. 93 (26) (2008) 263108.
[14] J. Fritz, M. Baller, H. Lang, H. Rothuizen, P. Vettiger, E. Meyer, H.-J. Güntherodt, C. Gerber, J. Gimzewski, Translating biomolecular recognition into nanomechanics, Science 288 (5464) (2000) 316–318.
[15] W. Pang, L. Yan, H. Zhang, H. Yu, E.S. Kim, W.C. Tang, Femtogram mass sensing platform based on lateral extensional mode piezoelectric resonator, Appl. Phys. Lett. 88 (24) (2006) 243503.
[16] H. Askari, H. Jamshidifar, B. Fidan, High resolution mass identification using nonlinear vibrations of nanoplates, Measurement 101 (2017) 166–174.
[17] K. Kiani, H. Ghaffari, B. Mehri, Application of elastically supported single-walled carbon nanotubes for sensing arbitrarily attached nano-objects, Curr. Appl. Phys. 13 (1) (2013) 107–120.
[18] D. Segall, S. Ismail-Beigi, T. Arias, Elasticity of nanometer-sized objects, Phys. Rev. B 65 (21) (2002) 214109.
[19] H. Üstünel, D. Roundy, T. Arias, Modeling a suspended nanotube oscillator, Nano Lett. 5 (3) (2005) 523–526.
[20] P. Vincent, S. Perisanu, A. Ayari, M. Choueib, V. Gouttenoire, M. Bechelany, A. Brioude, D. Cornu, S. Purcell, Driving self-sustained vibrations of nanowires with a constant electron beam, Phys. Rev. B 76 (8) (2007) 085435.
[21] K. Kiani, Free longitudinal vibration of tapered nanowires in the context of nonlocal continuum theory via a perturbation technique, Physica E 43 (1) (2010) 387–397.
[22] S. Hasheminejad, B. Gheshlaghi, Dissipative surface stress effects on free vibrations of nanowires, Appl. Phys. Lett. 97 (25) (2010) 253103.

[23] Y. Fu, H. Zhou, P. Zhang, Nonlinear free vibration of nanowires including size effects, Micro Nano Lett. 7 (4) (2012) 348–352.
[24] H. Askari, Nonlinear Vibration and Chaotic Motion of Uniform and Non-Uniform Carbon Nanotube Resonators (Ph.D. thesis), 2014.
[25] Q. He, C. Lilley, The vibration model and quality factor analysis of Timoshenko nanowires with surface stress, in: Nanotechnology (IEEE-NANO), 2012 12th IEEE Conference on, IEEE, 2012, pp. 1–6.
[26] A. Samaei, B. Gheshlaghi, G. Wang, Frequency analysis of piezoelectric nanowires with surface effects, Curr. Appl. Phys. 13 (9) (2013) 2098–2102.
[27] J. Wu, X. Li, A. Tang, K. Lee, Free and forced transverse vibration of nanowires with surface effects, J. Vib. Control 23 (13) (2017) 2064–2077.
[28] Y. Zhang, M. Pang, W. Chen, Transverse vibrations of embedded nanowires under axial compression with high-order surface stress effects, Physica E 66 (2015) 238 – 244.
[29] L. Jin, L. Li, Nonlinear dynamics of silicon nanowire resonator considering nonlocal effect, Nanoscale Res. Lett. 12 (1) (2017) 331.
[30] H. Sedighi, A. Bozorgmehri, Nonlinear vibration and adhesion instability of Casimir-induced nonlocal nanowires with the consideration of surface energy, J. Braz. Soc. Mech. Sci. Eng. 39 (2) (2017) 427–442.
[31] F. Khosravi, S.A. Hosseini, B.A. Hamidi, On torsional vibrations of triangular nanowire, Thin-Walled Struct. 148 (2020) 106591.
[32] Y. Yuan, K. Xu, K. Kiani, Torsional vibration of nonprismatically nonhomogeneous nanowires with multiple defects: Surface energy-nonlocal-integro-based formulations, Appl. Math. Model. 82 (2020) 17–44.
[33] A.D. Kerr, Elastic and viscoelastic foundation models, J. Appl. Mech. 31 (3) (1964) 491–498.
[34] J. Reddy, Nonlocal nonlinear formulations for bending of classical and shear deformation theories of beams and plates, Int. J. Eng. Sci. 48 (11) (2010) 1507–1518.
[35] S. Rao, Vibration of Continuous Systems, John Wiley & Sons, 2007.
[36] J. Reddy, Nonlocal nonlinear formulations for bending of classical and shear deformation theories of beams and plates, Internat. J. Engrg. Sci. 48 (11) (2010) 1507–1518.
[37] O. Bauchau, J. Craig, Euler–Bernoulli beam theory, in: O. Bauchau, J. Craig (Eds.), Structural Analysis, Springer Netherlands, Dordrecht, 2009, pp. 173–221.
[38] J. Peddieson, G. Buchanan, R. McNitt, Application of nonlocal continuum models to nanotechnology, Int. J. Eng. Sci. 41 (3) (2003) 305–312.
[39] S. Hosseini-Hashemi, I. Nahas, M. Fakher, R. Nazemnezhad, Nonlinear free vibration of piezoelectric nanobeams incorporating surface effects, Smart Mater. Struct. 23 (3) (2014) 035012.
[40] P. Soltani, A. Farshidianfar, Periodic solution for nonlinear vibration of a fluid-conveying carbon nanotube, based on the nonlocal continuum theory by energy balance method, Appl. Math. Model. 36 (8) (2012) 3712–3724.
[41] K. Kiani, Forced vibrations of a current-carrying nanowire in a longitudinal magnetic field accounting for both surface energy and size effects, Physica E 63 (2014) 27–35.
[42] B. Gheshlaghi, S. Hasheminejad, Vibration analysis of piezoelectric nanowires with surface and small scale effects, Curr. Appl. Phys. 12 (4) (2012) 1096–1099.
[43] H. Jiang, C. Wang, Y. Luo, Vibration of piezoelectric nanobeams with an internal residual stress and a nonlinear strain, Phys. Lett. A 379 (40) (2015) 2631–2636.
[44] D. Hodges, G. Pierce, Introduction to Structural Dynamics and Aeroelasticity, Vol. 15, Cambridge University Press, 2011.
[45] A.H. Nayfeh, D.T. Mook, Nonlinear Oscillations, John Wiley and Sons, 2008.
[46] A.H. Nayfeh, Introduction to Perturbation Techniques, John Wiley and Sons, 2011.
[47] N.E. Sanchez, The method of multiple scales: asymptotic solutions and normal forms for nonlinear oscillatory problems, J. Symb. Comput. 21 (2) (1996) 245–252.
[48] P. Ioannou, B. Fidan, Adaptive Control Tutorial, Society for Industrial and Applied Mathematics, 2006.
[49] S.-c. Wang, X.-g. Liang, X.-h. Xu, T. Ohara, Thermal conductivity of silicon nanowire by nonequilibrium molecular dynamics simulations, J. Appl. Phys. 105 (1) (2009) 014316.
[50] Y.-T. Yang, C. Callegari, X. Feng, K.L. Ekinci, M.L. Roukes, Zeptogram-scale nanomechanical mass sensing, Nano Lett. 6 (4) (2006) 583–586.
[51] J. Gieseler, L. Novotny, R. Quidant, Thermal nonlinearities in a nanomechanical oscillator, Nat. Phys. 9 (12) (2013) 806–810.
[52] J. Wang, Effect of temperature on elasticity of silicon nanowires, in: Key Engineering Materials, Vol. 483, Trans Tech Publ, 2011, pp. 526–531.
[53] S. Badu, S. Prabhakar, R. Melnik, Coarse-grained models of rna nanotubes for large time scale studies in biomedical applications, Biomedicines 8 (2020) 195.
[54] S. Badu, R. Melnik, S. Singh, Analysis of photosynthetic systems and their applications with mathematical and computational models, Appl. Sci. - Basel 10 (2020) 6821.
[55] S. Badu, S. Prabhakar, R. Melnik, Component spectroscopic properties of light-harvesting complexes with dft calculations, Biocell 44 (2020) 279 – 291.
[56] S. Badu, R. Melnik, S. Singh, Mathematical and computational models of rna nanoclusters and their applications in data-driven environments, Mol. Simul. 46 (2020) 1094 – 1115.
[57] S. Badu, S. Prabhakar, R. Melnik, Atomistic to continuum model for studying mechanical properties of rna nanotubes, Comput. Methods Biomech. Biomed. Eng. 23 (2020) 396 – 407.
[58] O. Malvar, E. Gil-Santos, J. Ruz, D. Ramos, V. Pini, M. Fernández-Regúlez, M. Calleja, J. Tamayo, A. San Paulo, Tapered silicon nanowires for enhanced nanomechanical sensing, Appl. Phys. Lett. 103 (3) (2013) 033101.
[59] S. Narendar, S. Gupta, S. Gopalakrishnan, Wave propagation in single-walled carbon nanotube under longitudinal magnetic field using nonlocal Euler–Bernoulli beam theory, Appl. Math. Model. 36 (9) (2012) 4529–4538.
[60] J. Kraus, Electromagnetics, McGrawHill, USA, 1984.
[61] L. Lew Yan Voon, B. Lassen, R. Melnik, M. Willatzen, Prediction of barrier localization in modulated nanowires, J. Appl. Phys. 96 (2004) 4660 – 4662.
[62] S. Prabhakar, R. Melnik, L.L. Bonilla, Coupled multiphysics, barrier localization, and critical radius effects in embedded nanowire superlattices, J. Appl. Phys. 113 (2013) 244306.
[63] M. Alvaro, L.L. Bonilla, M. Carretero, R.V.N. Melnik, S. Prabhakar, Transport in semiconductor nanowire superlattices described by coupled quantum mechanical and kinetic models, J. Phys. - Condens. Matter 25 (2013) 335301.
[64] A.K. Tiwari, R. Melnik, Non-local optical response of nanowire-film system: effect of geometric parameters, J. Coupled Syst. Multiscale Dyn. 5 (2017) 212 – 216.
[65] R. Dhote, R. Melnik, J. Zu, Dynamic multi-axial behavior of shape memory alloy nanowires with coupled thermo-mechanical phase-field models, Meccanica 49 (2014) 1561 – 1575.
[66] H. Du, X. He, L. Wang, R. Melnik, Analysis of shape memory alloy vibrator using harmonic balance method, Appl. Phys. A - Mater. Sci. Process. 126 (2020) 568.